Hydrol. Earth Syst. Sci., 17, 3077–3094, 2013
www.hydrol-earth-syst-sci.net/17/3077/2013/
doi:10.5194/hess-17-3077-2013

Hydrology and Earth System Sciences
Open Access

A framework for evaluating regional hydrologic sensitivity to climate change using archetypal watershed modeling

S. R. Lopez[1,*], **T. S. Hogue**[1,*], **and E. D. Stein**[2]

[1]Department of Civil and Environmental Engineering, University of California, Los Angeles, USA
[2]Southern California Coastal Water Research Project, Costa Mesa, CA, USA
[*]now at: Colorado School of Mines, Golden, CO, USA

Correspondence to: T. S. Hogue (thogue@mines.edu)

Received: 5 October 2012 – Published in Hydrol. Earth Syst. Sci. Discuss.: 14 December 2012
Revised: 29 March 2013 – Accepted: 20 June 2013 – Published: 1 August 2013

Abstract. The current study focuses on the development of a regional framework to evaluate hydrologic and sediment sensitivity, at various stages of urban development, due to predicted future climate variability. We develop archetypal watersheds, which are regional representations of observed physiographic features (i.e., geomorphology, land cover patterns, etc.) with a synthetic basin size and reach network. Each of the three regional archetypes (urban, vegetated and mixed urban/vegetated land covers) simulates satisfactory regional hydrologic and sediment behavior compared to historical observations prior to a climate sensitivity analysis. Climate scenarios considered a range of increasing temperatures, as estimated by the IPCC, and precipitation variability based on historical observations and expectations. Archetypal watersheds are modeled using the Environmental Protection Agency's Hydrologic Simulation Program–Fortran model (EPA HSPF) and relative changes to streamflow and sediment flux are evaluated. Results indicate that the variability and extent of vegetation play a key role in watershed sensitivity to predicted climate change. Temperature increase alone causes a decrease in annual flow and an increase in sediment flux within the vegetated archetypal watershed only, and these effects are partially mitigated by the presence of impervious surfaces within the urban and mixed archetypal watersheds. Depending on the extent of precipitation variability, urban and moderately urban systems can expect the largest alteration in flow regimes where high-flow events increase in frequency and magnitude. As a result, enhanced wash-off of suspended sediments from available pervious surfaces is expected.

1 Introduction

Numerous reports by the Intergovernmental Panel on Climate Change (1992, 1995, 2001 and 2007) predict global mean temperatures to increase from 1.4 to 5.8 °C over the next 100 yr. Atmospheric warming will impact regional rainfall patterns, snow accumulation and melt, river runoff, soil moisture storage and plant water availability (McCabe and Wolock, 2008; Costa and Soares, 2009; Githui et al., 2009; Hidalgo et al., 2009; Kunkel et al., 2009; Clark, 2010; Wang et al., 2010). There is significant motivation to perform regional studies investigating the effects of climate change on local water resources, especially in water-stressed regions (Mote et al., 2005; CCCC, 2006; Aragão et al., 2007; Westerling and Bryant, 2008). In the southwestern United States, potential and observed impacts of climate change have been summarized by numerous research efforts (Knowles and Cayan, 2002; Kiparsky and Gleick, 2003; Miller et al., 2003; Hayhoe et al., 2004; Kim, 2005; Mote et al., 2005; CAT, 2009). Several studies have focused on addressing climate change and impacts to water resources in snow-prevalent regions of northern California (Gleick and Chalecki, 1999; Christensen et al., 2004; Hayhoe et al., 2004; Mote et al., 2005; McCabe and Wolock, 2008); however, few studies have evaluated climate impacts in southern California, a region with rapidly expanding metropolitan areas and a projected population growth of 40 % by 2050 (California Department of Finance, 2007). The region is also heavily dependent on imported water to satisfy growing water demands (LADWP, 2010; Pataki et al., 2011). A range of regional projects are being developed to promote local sustainability

and promote groundwater infiltration and reuse. However, potential water resource losses due to climate change will ultimately strain and hamper efforts to make the region more locally sustainable.

The traditional approach for predicting future large-scale climate response is through the use of general circulation models (GCMs) (10–100 km^2); however, these coarse resolution models are incapable of resolving regional- to local-scale processes that are relevant to societal concerns and local decision making (e.g., water quality and availability, energy use, air quality, storm severity, etc.). Efforts to use GCM output at the local or watershed scale have led to the development of statistical (using historical and GCM output) and dynamic (using GCM output and coupled regional models) downscaling methods. Although both these approaches have advantages, the additional effort associated with these methods may not necessarily result in improved prediction of the daily time step or capture localized effects (i.e., orography).

A range of simple approaches have been developed to evaluate potential change in runoff and sedimentation, including performing sensitivity analyses on watershed systems and varying parameters such as land cover, precipitation, temperature and evapotranspiration (DeWalle and Swistock, 2000; Pruski and Nearing, 2002; Singer and Dunne, 2004; Nearing et al., 2005; Soboll, 2011). This approach does not require advanced statistical methodologies or extensive computing. Random variability (wet day frequency and precipitation amount) is generally added to the precipitation time series, whereas an increase or decrease in temperature range is added to historical temperature. By altering historical time series, the user is able to develop relatively robust scenarios to evaluate watershed hydrologic and sediment response due to expected variability in climate.

The goals of this work are to (a) develop a user-friendly and efficient framework for regional hydrologic analysis, to (b) assess hydrologic and sediment behavior sensitivity to climate variability within a quasi-synthetic framework, and to (c) analyze how varying levels of urbanization affect the potential changes to flooding and sediment transport in southern California. We address these goals by developing regional quasi-synthetic watershed archetypes based on observed regional physiographic features and evaluating the effects of varying climate on runoff and sediment flux in the developed archetypes. We also employ an operational environmental and water resource model, the Hydrologic Simulation Program–Fortran (HSPF), that has been used extensively across southern California (Ackerman et al., 2005; Bandurraga, 2011; He and Hogue, 2011; Hevesi et al., 2011). A range of studies have used synthetic watersheds for understanding hydrologic behavior (Smith and Eli, 1995; Manguerra and Engel, 1998; Moradkhani et al., 2005; Goff and Gentry, 2006). Alternatively, we develop a quasi-synthetic approach for regional archetypes that use observed regional physiographic features (i.e., geomorphology, land cover patterns, etc.) and synthetic derivation of basin and reach networks. Each regional archetype simulates representative short-term (daily) and long-term (annual) hydrologic and sediment behavior prior to the climate sensitivity analysis. Our work deviates from traditional methods because it obtains information beyond a single watershed-scale analysis and also avoids use of a macro-scale hydrologic model that requires extensive input information (i.e., variable infiltration capacity macroscale hydrologic model). The developed approach can be readily applied to address similar objectives in other regions of the United States.

2 Methods

2.1 Study region and data

The selected study area is the southern California coast, from south of Santa Barbara to the US–Mexico Border. The region is characterized by a Mediterranean-type climate with precipitation ranging from 15 to 102 cm and mean annual temperature ranging from 16 to 18 °C (Levien et al., 2002). Lower elevation vegetation (below 1800 m) is predominantly chaparral and scrubs, while forested communities are found at elevations above 1800 m (Levien et al., 2002). Counties within southern California also have varying levels of urban and built-up land ranging from 32 to 91 % (California Department of Conservation – Division of Land Resource Protection, 2011).

Observed physiographic information including land cover, soil type, drainage area, channel length and channel slope were gathered for selected coastal southern California watersheds (Table 1). Land cover distribution was obtained using the NOAA Coastal Change Assessment Program (CCAP) data, which are based on 30 m LANDSAT imagery (NOAA-CSC, 2003). The data were originally classified into 39 land types from CCAP; however, extensive land cover classifications were unnecessary for the purpose of this project. Similar classifications (i.e., chaparral and chaparral park, sage and sage park, etc.) were combined resulting in 23 land cover types.

The observed distribution of physiographic properties as well as regional climate patterns (Nezlin and Stein, 2005) were used to subset the study area into three regions (for three proposed archetypes): Region I includes Ventura County watersheds with minimal urbanization vegetated with scrub/shrub, sage and chaparral (typical plant type in southern California), Region II represents the Los Angeles region with relatively dense urbanization and little natural land cover, and Region III spans the San Diego area which has an observed mix of vegetated and urban land types (Fig. 1). The mean urban land cover (total of low residential, high residential and commercial types) is 7, 58 and 22 % within Regions I, II and III, respectively. Mean vegetated land cover (shrub/sage/chaparral, forest, grass and agriculture) for Regions I, II and III are 90, 39 and 75 %,

Table 1. Physiographic parameters were obtained for 11 coastal watersheds (*) including drainage area, channel length, slope, land cover (percent urban provided) and reach/channel parameters (NOAA-CSC, 2003). Hydrologic (USGS, 2011) and sediment data (USGS, 2009) were extracted from available watersheds within the archetypal regions.

Archetype Region	Watersheds Represented	Drainage Area [km^2]	Channel Length [m]	Slope [-]	Percent Urban	USGS Station ID	Hydrologic Data Start Date	Hydrologic Data End Date	Sediment Data Start Date	Sediment Data End Date
I	Arroyo Simi	183				11105850	1/1/1955	9/30/1983	10/1/1968	9/30/1978
	Calleguas*	642	46175	0.021	15.2	11106550	1/1/1969	12/31/2005	10/1/1968	9/30/1978
	Malibu*	272	28034	0.012	9.1	11105500	1/1/1955	9/30/1979	–	–
	Santa Clara*	1619	106612	0.016	2.4	11109000	10/1/1996	12/31/2005	10/1/1968	9/30/1978
	Santa Ynez	2044				11133000	1/1/1955	12/31/2005	–	–
	Topanga*	47	10433	0.033	0.7	11104000	–	–	–	–
	Ventura	487				11118500	–	–	10/1/1968	9/30/1971
									11/1/1971	6/30/1972
									10/1/1972	9/30/1973
									10/1/1974	9/30/1981
									10/1/1985	9/30/1986
II	Ballona*	233	14284	0.01	76.0	11103500	1/1/1955	9/30/1978	–	–
	Los Angeles – Long Beach	2142				11103000	1/1/1955	9/30/1992	–	–
	Los Angeles – Sepulveda Dam	409				11092450	1/1/1955	12/31/2005	–	–
	Rio Hondo	236				11101250	3/1/1956	12/31/2005	–	–
	San Gabriel*	1656	59691	0.025	39.2	11088000	–	–	–	–
	Santa Ana	4403				11078000	–	–	10/1/1981	9/30/1987
	Santa Ana/Nr Anaheim	1619				11075600	–	–	10/1/1972	9/30/1977
III	Los Coches	32				11022200	10/1/1983	12/31/2005	10/1/1972	9/30/1974
	Pueblo SD*	113	11140	0.012	80.4	–	–	–	–	–
	San Diego – Fashion*	1111	68809	0.014	13.2	11023000	1/1/1983	12/31/2005	10/1/1983	9/30/1984
	San Diego – Santee	976				11022500	–	–	10/1/1969	9/30/1978
	San Dieguito*	875	56494	0.016	6.7	11030500	–	–	10/1/1983	9/30/1984
	San Luis Rey*	1329	106454	0.015	3.7	11042000	1/1/1967	12/31/2005		
	Santa Margarita*	1917	91309	0.018	4.1	11046000	–	–	10/1/1968	9/30/1971
	Santa Maria	149				11028500	1/1/1955	12/31/2005	10/1/1977	9/30/1978
	Santa Ysabel	290				11025500	1/1/1955	12/31/2005		
	Sweetwater	118				11015000	1/1/1983	12/31/2005		

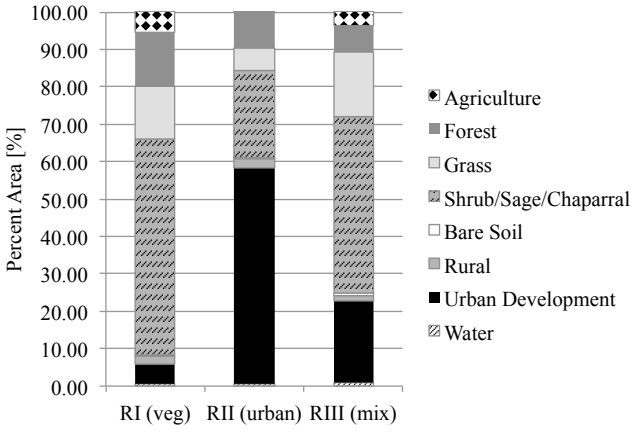

Fig. 1. Percent of total area of aggregated land cover distributions for Regions I–III.

respectively. Distinguished by climate and land cover differences, the three systems along the coastline are defined as vegetated (Region I), urban (Region II) and mixed (Region III).

A time series of representative climatology was gathered for each defined region. Based on prior work in southern California (Nezlin and Stein, 2005), we advocate that selecting a gauge within each distinct region provides reasonable estimation of climatology for each defined study area. Hourly meteorological observations from proximal airport stations within each region were used: Santa Maria (CA007946), Los Angeles International (CA005114) and San Diego (CA007740) (EPA, 2009). Each time series contains precipitation, temperature and related meteorological variables from 1 January 1950 to 31 December 2005 (55 yr). Within this time frame there was substantial interannual variability, with 16 El Niño events and 18 La Niña events (NOAA-NWS, 2010). Historical flow and sediment concentration data (USGS, 2009) were also gathered from area watersheds (Table 1) for classification of the regional systems as well as for model evaluation.

2.2 Development of archetypal watersheds

Each archetypal watershed was developed to serve as a representative model for that region and provide reasonable simulations of hydrologic and suspended sediment loads within the framework. Observed datasets (climate, physiology, hydrology and sediment) were used to develop the archetypes and establish the physical construct (Fig. 2). Mean regional land cover and slope were directly integrated

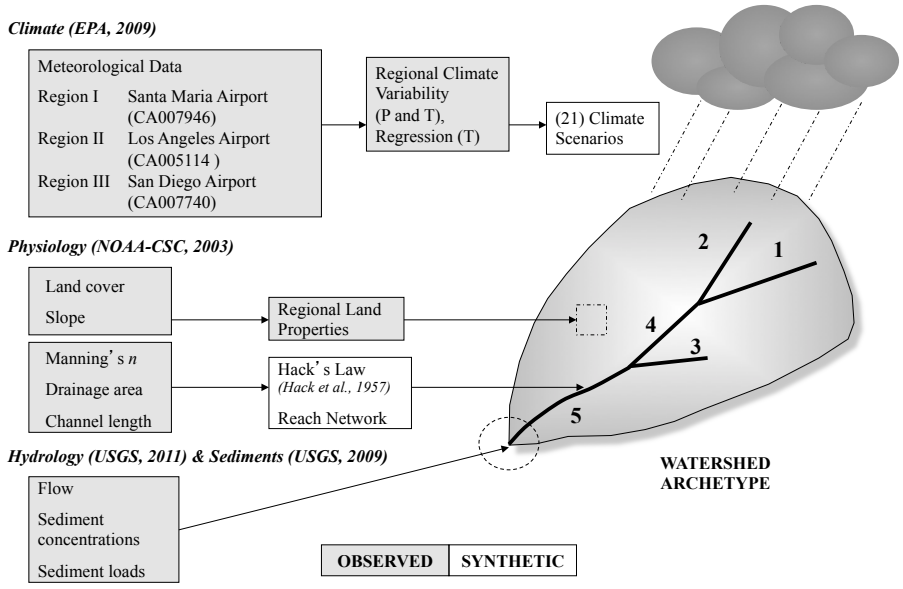

Fig. 2. Methodology for development of regional watershed archetypes. Shaded boxes indicate the usage of observed meteorological, land cover and hydrologic data (sources listed); non-shaded boxes indicate the usage of empirical and/or synthetic approaches.

into developing the archetype; however, the large variability in channel length, drainage size and reach network led to the exploration of more synthetic approaches for these parameters. The drainage area (259 km^2; 100 mi^2) and number of reaches (5) were held constant for each archetype in order to constrain variability in system response due to size and reach distribution. A synthetic channel length (distance from watershed outlet to farthest point on the main channel) was obtained using Hack's law (Eq. 1), an empirical relationship between the length of the longest stream [L: miles] and drainage area [A: square miles] (Hack et al., 1957) and defined as

$$L = 1.4A^{0.6}. \quad (1)$$

Using the archetypal watershed area of 259 km^2 and the corresponding total channel length of 35.8 km, the remaining reach properties were designed based on evaluation and general knowledge of typical drainage systems in southern California. Reaches 1, 2, 4 and 5 were set at one-third the total channel length (11.9 km) and reach 3 was set at one-sixth the total channel length (6 km). Reaches 2, 4 and 5 are considered the main channel and reaches 1 and 3 are contributing to the stream network (Fig. 2). Contributing drainage area for each reach is set at one-sixth the total area with the exception of reach 5, the outlet stream, which is assumed to be one-third the entire basin. The change in elevation for each reach is a function of the reach length and the overall slope of the channel based on slope measurements within each respective region (Table 1). Manning's roughness coefficient for overland flow (NSUR) for pervious and impervious surfaces was 0.2 and 0.1, respectively, for all watersheds. These surface coefficients have also been used in the HSPF model for southern California (He and Hogue, 2011; Ackerman, 2005). The Manning's n channel coefficient for each region was determined based on the predetermined land cover classification. Region I's channels are assumed primarily natural ($n = 0.04$), Region II channels are cement ($n = 0.01$) and Region III Manning's n is a mixture of cement and natural reaches ($n = 0.025$). Model sensitivity for Manning's n was primarily noted with the channel coefficient.

2.2.1 Archetypal model assumptions

The vegetated archetypal watershed (Region I) represents areas with a higher percentage of pervious land cover, which generally promotes surface infiltration and reduces streamflow. Sediment yield is expected to be higher in the vegetated archetypal system because increasing urbanization has been shown to decrease erosion locally (Wolman, 1967; Trimble, 1997). The urban archetypal watershed (Region II) should exhibit more intense, high-flow output and low sediment flux, characteristic of urban watersheds with cement-lined channel systems. Streambed erosion from the remaining natural channels can be accelerated in urban systems if the frequency and magnitude of peak discharge increases due to runoff from impervious surfaces (Trimble, 1997). Region III's archetypal watershed is considered an area that is increasing in urbanization and may experience sediment and flow patterns that reside between the vegetated and fully urbanized systems, with smaller flows than the urban archetype and lower sediment loads than the vegetated system. No dams or upstream obstructions were integrated into the archetypal models in this initial work. Changes to land

cover are not explored within this study because the archetypal systems are designed to represent the current range of urbanization patterns in southern California.

2.3 Model description

The Hydrologic Simulation Program–Fortran (HSPF) simulates watershed hydrology and movement of contaminants including fate and transport of sediment, pesticides, nutrients and other water quality parameters in stream systems (Bicknell et al., 2000). The HSPF model was selected because it has been used in previous studies conducted in southern California counties – Ventura (Bandurraga, 2011), San Bernardino (Hevesi et al., 2011) and Los Angeles (Ackerman et al., 2005; He and Hogue, 2011) – and is used by the EPA for watershed investigations.

Precipitation, temperature and estimations of potential evaporation are required inputs for HSPF. Three modules are needed for simulation of watershed hydrology: PERLND, IMPLND and RCHRES. The PERLND (pervious surfaces) and IMPLND (impervious surfaces) modules require land cover classification and several geo-physical characteristics and RCHRES (streams) requires physical dimensions (length, slope, roughness coefficient, channel shape, etc.) and the stream network to estimate discharge (Bicknell, 2000; Singh et al., 2005). Use of HSPF requires division of the watershed into land segments (based on land cover) and river reaches. Partitioning of surface runoff/infiltration is governed by the Philips equation (Philips, 1957). Runoff then moves laterally to downslope segments or to a river reach or reservoir. Other simulated processes include interception, percolation, interflow and groundwater movement. The HSPF applies Manning's equation for routing overland flow and kinematic wave for channel routing.

Sediment simulation is performed using three modules: SEDMNT (pervious surfaces), SOLIDS (impervious surfaces) and SEDTRN (stream transport). Sediment from pervious land cover detaches the soil surface and enters the stream result via overland flow (Bicknell, 2000). Solids from impervious surfaces wash off due to a precipitation event; the load is primarily driven by the rate of accumulation of solid materials (Bicknell, 2000). Stream sediments are initialized by specifying clay, silt and sand fractions, and result from processes such as deposition, scour and transport (Bicknell, 2000). Summation of sediments from all three modules results in the total sediment load.

Modeling was undertaken for all archetypal watersheds using the following datasets: historical observations (1955–2005) and 21 Climate Scenarios (50 yr period) (described in Sect. 2.4). A 5 yr spin-up period (not used in final analysis) was included in all model simulations. The model was run at an hourly time step using the meteorological data from the three proximal airport stations for each region.

2.3.1 Parameter selection

PERLND and IMPLND hydrology parameter values were initialized using previous work conducted on southern California watersheds with HSPF (He and Hogue, 2011; Ackerman et al., 2005). Hydrology parameters were established first, prior to sediment calibration, by comparing simulated flow to observations from watersheds within the three study regions. The list of watersheds and hydrologic data gathered from the United States Geological Survey (USGS, 2011) are provided in Table 1. Daily observations were used to assure model behavior was within regional expectations; however, parameter selection was based on each archetypal system's ability to estimate mean monthly and annual flow behavior (over the same data period). Model performance was assessed using root-mean-square error (RMSE), Nash–Sutcliffe efficiency (NSE), percent bias (BIAS) and Pearson's correlation coefficient (R^2) (Eqs. 2–5):

$$\mathrm{RMSE} = \sqrt{\frac{1}{n}\sum_{t=1}^{n}(Q_{\mathrm{sim},t} - Q_{\mathrm{obs},t})^2}, \tag{2}$$

$$\%\mathrm{BIAS} = \left(\frac{\sum_{t=1}^{n}\left(Q_{\mathrm{sim},t} - Q_{\mathrm{obs},t}\right)}{\sum_{t=1}^{n}\left(Q_{\mathrm{obs},t}\right)}\right) \times 100, \tag{3}$$

$$\mathrm{NSE} = 1 - \left(\frac{\sum_{t=1}^{n}(Q_{\mathrm{sim},t} - Q_{\mathrm{obs},t})^2}{\sum_{t=1}^{n}(Q_{\mathrm{obs},t} - \bar{Q}_{\mathrm{obs}})^2}\right), \tag{4}$$

$$R^2 = \left(\frac{n\sum_{t=1}^{n} Q_{\mathrm{sim},t}Q_{\mathrm{obs},t} - (\sum_{t=1}^{n} Q_{\mathrm{sim},t})(\sum_{t=1}^{n} Q_{\mathrm{obs},t})}{\sqrt{(n-1)(\sum_{t=1}^{n} Q_{\mathrm{sim},t}^2) - (\sum_{t=1}^{n} Q_{\mathrm{sim},t})^2}\sqrt{(n-1)(\sum_{t=1}^{n} Q_{\mathrm{obs},t}^2) - (\sum_{t=1}^{n} Q_{\mathrm{obs},t})^2}}\right)^2. \tag{5}$$

For each of the above formulations, Q_{sim} is the simulated flow, Q_{obs} is the observed flow, $\bar{Q}_{\mathrm{obs}}$ is the overall mean observed flow, n is the total number of observations, and t is the time step used for statistical comparison. Annual comparisons were also made using long-term runoff ratios from observed and archetypal watersheds.

Observed suspended-sediment and flow data (Table 1) were compared to archetypal simulations using log–log (concentration–discharge) rating curves. Rating curves were fitted using a second-order linear regression, and 95 % confidence intervals from the archetypal rating curve were compared to observations. Sediment parameters were obtained using calibration steps suggested by Bicknell (2000) and Donigian and Love (2003). Rating curves were used to compare long-term sediment simulations instead of performing analysis on a storm-by-storm basis. An initial shortcoming in calibrating sediment was availability of long-term observations. In order to be confident in the long-term simulations

Table 2. Final model parameters used for discharge simulations in archetypal watersheds.

Label			Region I	Region II	Region III
	Description	Units	Veg.	Urban	Mix
Pervious Parameters					
AGEWTP	Fraction of Remaining E–T From Active Ground Water Storage	–	0	0	0
AGWRC	Basic Ground Water Recession Rate	d^{-1}	0.99	0.99	0.99
BASETP	Fraction of Remaining E–T From Base Flow	–	0.04	0	0.06
CEPSC	Interception Storage Capacity	cm	0.25	0.25	0.25
DEEPFR	Fraction of Ground Water to Deep Aquifer	–	0.2	0.1	0.5
FOREST	Forest Fraction	–	0.11	0.1	0.07
INFEXP	Infiltration Equation Exponent	–	2	2	2
INFILD	Ratio Between the Maximum and Mean Infiltration Capacities	–	2	2	2
INFILT	Infiltration Capacity	$cm\,h^{-1}$	0.64	0.33	0.51
INTFW	Interflow Inflow Parameter	–	2	0.7	1.125
IRC	Interflow Recession Parameter	d^{-1}	0.5	0.5	0.5
KVARY	Ground Water Recession Flow Coefficient	cm^{-1}	1.97	0.39	1.18
LSUR	Overland Flow Length	m	91	91	91
LZETP	Lower Zone E–T Parameter	–	0.7	0.1	0.5
LZSN	Lower Zone Nominal Storage	cm	40.64	35.56	38.10
NSUR	Manning's n for Overland Flow	–	0.2	0.2	0.2
PETMAX	Temperature Maximum for Evapotranspiration (E–T)	°C	4.4	4.4	4.4
PETMIN	Temperature below which E–T will be zero	°C	1.7	1.7	1.7
SLSUR	Overland Flow Slope	–	0.019	0.017	0.015
UZSN	Upper Zone Nominal Storage	cm	3.56	2.87	3.34
Impervious Parameters					
LSUR	Overland Flow Length	m	91	91	91
NSUR	Manning's n for Overland Flow	–	0.01	0.01	0.01
PETMAX	Temperature Maximum for E–T	°F	40	40	40
PETMIN	Temperature That E–T is Zero	°F	35	35	35
RETSC	Retention Storage Capacity of the Surface	cm	0.15	0.17	0.15
SLSUR	Slope	–	0.019	0.017	0.015

of mean annual sediment flux ($ton\,yr^{-1}$), simulations were also compared to observations provided by Inman and Jenkins (1999) for the 1969–1995 data period.

Final parameter values for hydrologic and sediment simulations are summarized in Tables 2 and 3. The vegetated archetypal watershed (Region I) in our study required the separation of the coefficient (KRER) and exponent (JRER) of the soil detachment equation in order to obtain reasonable sediment estimates based on observed results. The change in these parameter values was applied to chaparral and sage land covers, the two dominant natural land cover types in Region I.

2.4 Development of climate scenarios

To evaluate each archetypal watershed's sensitivity to climate variability, historical precipitation and temperature time series were perturbed to serve as input to the HSPF model within each region. Changes to temperature were based on regression analysis using long-term observations (first-order regression) and potential increases in temperature (IPCC, 2007). The precipitation scenarios involved altering the frequency and duration by adding variability to the observed hourly time series. The combination of temperature and precipitation scenarios led to the development of 21 climate ensembles (Table 4). The developed scenarios were then run through HSPF for each archetypal watershed to evaluate the impact of precipitation variability and temperature increase (details of the developed climate scenarios are outlined in Sects. 2.4.1–2.4.3). Modeling simulations were generated at the hourly time step to evaluate changes to peak storm discharge, storm volume and storm sediment recurrence interval.

2.4.1 First-order temperature regression

A first-order regression analysis was performed using the historical (WY1955-2005) minimum and maximum temperature observations from the three proximal airport locations. Using the regression coefficients, integral increases in

Table 3. Final model parameters used for sediment simulations in archetypal watersheds.

				Region I	Region II	Region III
	Name	Definition	Units	Veg.	Urban	Mix
SEDMNT						
	SMPF	Management practice (P) factor from USLE	–	0.8	0	0.7
	KRER	Coefficient in the soil detachment equation	complex	0.7	0.1	0.5
Chaparral	KRER			0.6		
Sage	KRER			0.6		
	JRER	Exponent in the soil detachment equation	–	1	1	1
Chaparral	JRER			1.2		
Sage	JRER			1.2		
	AFFIX	Daily reduction in detached sediment	d^{-1}	0.03	0.03	0.03
	COVER	Fraction land surface protected from rainfall	–	0.88	0.88	0.88
*	NVSI	Atmospheric additions to sediment storage	kg ac-day^{-1}	0	0	0
	KSER	Coefficient in the sediment wash-off equation	complex	8	0.5	2
	JSER	Exponent in the sediment wash-off equation	–	0.53	2	0.45
	KGER	Coefficient in the soil matrix scour equation	complex	1	0.01	0.6
	JGER	Exponent in soil matrix scour equation	–	2	1	1.5
				Region I	Region II	Region III
	Name	Definition	Units	Veg.	Urban	Mix
SOLIDS						
	KEIM	Coefficient in the solids wash-off equation	complex	0.3	0.02	0.6
	JEIM	Exponent in the solids wash-off equation	–	1.5	1	2
	ACCSDP	Solids accumulation rate on the land surface	kg ac-day^{-1}	0.23	0.45	0.45
	REMSDP	Fraction of solids removed per day	d^{-1}	0.03	0.03	0.03

* NVSI is the rate sediment enters the detached sediment storage from the atmosphere. A negative value simulates sediment removal (i.e., via wind, or anthropogenically).

Table 4. Description of climate scenarios evaluated.

Temperature increase	Precipitation increase [%]					#
[°C]	0	5	10	25	50	Scenarios
0.5	√	√	√	√	√	5
1	√	√	√	√	√	5
2	√	√	√	√	√	5
3	√	√	√	√	√	5
First-order regression	√					1
Total						21

* Trend increase for Regions I–III is 1.69, 1.37 and 1.13 °C, respectively.

minimum and maximum temperature were applied over the 50 yr data period. Final (average) increases in temperature were 1.69, 1.37 and 1.13 °C in Regions I, II and III, respectively, for the 50 yr period.

2.4.2 Temperature increase based on IPCC estimations

The IPCC AR4 Synthesis Report (2007) estimates an increase of 1.4 to 5.8 °C by 2100 depending on emission scenario and global location. Since the simulation length spans half of the IPCC (100 yr) period, temperature increase scenarios were based on the assumption that temperature increases would range from 0.5 to 3 °C in the study area. Incremental increases of 0.5, 1, 2 and 3 °C were applied to minimum and maximum temperatures time series for each region.

2.4.3 Precipitation variability

Linear regression of historical precipitation data indicated a slight increase in precipitation, but the observed trends were not significant (ANOVA; $p = 0.05$). However, various studies note that an increase in variability of annual precipitation may be expected as a result of climate change (Rind et al., 1989; Meehl et al., 2000; DWR, 2006). Consequently, random, normally distributed variability was added to storm periods within the historical precipitation records. The randomization to the historical series altered precipitation duration and storm intensity. Archetypal watersheds experienced a 5, 10, 25 and 50 % increase in the variability (normal distribution) of precipitation. The derived precipitation scenarios were combined with the temperature scenarios from Sect. 2.4.2 to produce climate ensembles with various

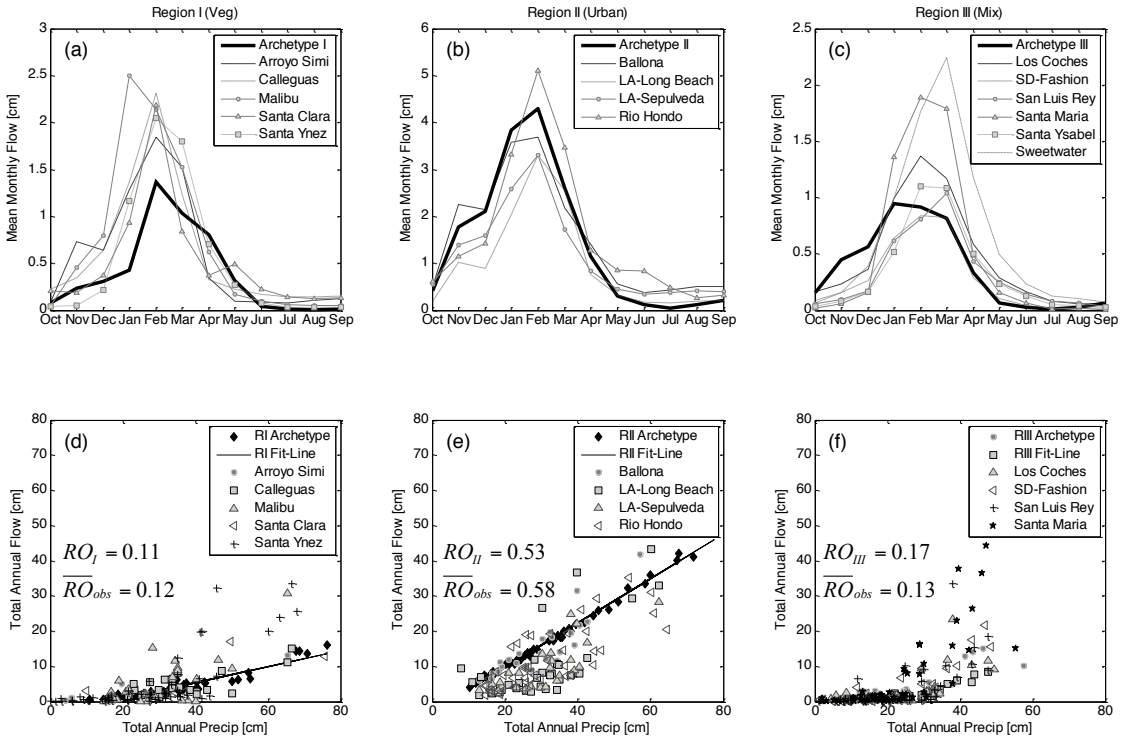

Fig. 3. Archetypal comparisons of mean monthly flow behavior **(a–c)** and total annual flow versus annual precipitation **(d–f)** for each respective region.

combinations of increasing temperatures (IPCC) and increasing precipitation uncertainty (variability) (Table 4). The 10, 25, 50, 75 and 90 % probability peak flow values were only identified for scenarios involving precipitation variability; and these were evaluated at the 2, 35 and 50 yr recurrence intervals.

3 Results

3.1 Regional precipitation and temperature trends

Using the selected airport gauges, long-term precipitation and temperature trends were examined for each region for 1950–2005. Region II (urbanized) experienced the highest precipitation variability (208.4 cm^2) compared to Region I (177.9 cm^2) and Region III (108.0 cm^2). Mean annual precipitation for this data period is 33.3, 31.8 and 25.1 cm, respectively by region. The mean annual temperature in the highly vegetated region, Region I, was relatively lower (56.8 °C) compared to the urban Region II (62.7 °C) and mixed III (63.6 °C). Temperature trends in all three regions were noted to be significant ($p < 0.5$), while precipitation trends were not.

3.2 Archetypal evaluation: baseline period runoff

Hydrologic data from five watersheds were extracted from Region I and evaluated against simulated flow from the archetypal watershed (Table 5). Simulations from the Region I archetype provided fair representation of regional watershed behavior. Average statistics (RMSE = 4.35 cm, NSE = 0.62; $R^2 = 0.79$) indicate the model reasonably simulates mean monthly flow behavior, with best performance observed for the smallest watershed system (Arroyo Simi). Overall accuracy is slightly reduced during peak flow months (January–March) when compared to most of the region's watersheds. Attempts to increase peak discharge behavior for the winter months resulted in consistently higher flows throughout the year and somewhat reduced accuracy in simulating low-flow behavior. This also reduced sediment concentrations to below observed ranges. Hence, derivation of our final parameters values involved giving appropriate weight to low-flow accuracy while maintaining adequate peak discharge simulation. For Region II, the mean monthly trends (Fig. 3b) closely match overall observations in the region with relatively high NSE (0.82) and R^2 (0.95). There is slight oversimulation during the winter and spring seasons for some watersheds (% BIAS = 8.74), but simulations are generally within the range of the long-term observations. Overall statistics and visual inspection indicate model simulations for Region III capture low-flow regimes better than in

Table 5. Hydrologic statistics comparing mean monthly flow depth of observations and archetypal outputs for the same observed period. Runoff ratios are calculated using total annual precipitation and flow depth for each watershed.

	Region I	Start Date	Stop Date	RMSE [cm]	NSE	% BIAS	R^2	Runoff Ratio
1	Arroyo Simi	1/1/1955	9/30/1983	2.82	0.80	−13.75	0.90	0.11
2	Calleguas	1/1/1969	12/31/2005	4.03	0.65	−32.33	0.72	0.09
3	Malibu	1/1/1955	9/30/1979	7.55	0.25	−60.76	0.67	0.26
4	Santa Clara	10/1/1996	12/31/2005	3.27	0.69	−25.41	0.73	0.06
5	Santa Ynez	1/1/1955	12/31/2005	4.06	0.69	−36.02	0.93	0.10
	Average			4.35	0.62	−33.66	0.79	0.12
	Region II							
1	Ballona	1/1/1955	9/30/1978	2.29	0.97	−13.14	0.98	0.62
2	Los Angeles – Long Beach	1/1/1955	9/30/1992	6.34	0.65	39.66	0.91	0.51
3	Los Angeles – Sepulveda Dam	1/1/1955	12/31/2005	4.86	0.75	17.23	0.98	0.54
4	Rio Hondo	3/1/1956	12/31/2005	4.88	0.90	−8.77	0.90	0.64
	Average			4.59	0.82	8.74	0.94	0.58
	Region III							
1	Los Coches	10/1/1983	12/31/2005	1.82	0.85	−27.70	0.93	0.23
2	San Luis Rey	1/1/1983	12/31/2005	1.94	0.62	34.25	0.92	0.10
3	Santa Maria	1/1/1967	12/31/2005	1.06	0.90	6.62	0.96	0.14
4	Santa Ysabel	1/1/1955	12/31/2005	3.35	0.79	−22.56	0.90	0.09
5	San Diego (Fashion)	1/1/1955	12/31/2005	0.72	0.97	5.86	0.97	0.11
6	Sweetwater	1/1/1983	12/31/2005	4.53	0.62	−45.63	0.95	0.20
	Average			2.32	0.78	–4.29	0.94	0.13

Region I and II (RMSE = 2.32 cm) and overall simulations generally reside within the range of flow observations (Table 5). There is a slight undersimulation of peak behavior (%BIAS = −4.29), but there is still a strong correlation to observations ($R^2 = 0.94$) and reasonable overall model performance (NSE = 0.78).

Emphasis was placed on capturing annual long-term observations, in addition to monthly streamflow trends. Runoff ratios (annual runoff depth/annual precipitation depth) were calculated for the archetypal watersheds and compared to regional values (Table 5). The runoff ratio provides an estimate of the amount of precipitation leaving a system as surface flow and how much is lost to other processes (i.e., evaporation/evapotranspiration, infiltration, etc.). Region I's archetype model (vegetated) simulates a relatively low average runoff ratio, 0.11, which is within the observed range for Region I and just above the mean runoff ratio (0.12). The Malibu and Santa Ynez watersheds have higher runoff ratios during years where observed annual precipitation exceeds the mean (approximately 40 cm) (Fig. 3d). A potential reason for this behavior may be the amount of urbanization in these watersheds that slightly exceeds the archetype, promoting higher runoff behavior.

The runoff ratio for Region II's archetypal model is 0.53 due to the higher impervious land cover. The simulated value closely matches the mean observed ratio for the region (0.58). The archetypal model oversimulates in comparison to the Los Angeles sites (Long Beach and Sepulveda Dam; Table 5 and Fig. 3e), especially for events less than the mean annual precipitation (40 cm). However, our simulation does capture the long-term runoff trends of the Rio Hondo and Ballona watersheds, which are physically more similar to our Region II archetype in area (236 and 233 km^2, respectively) and urban development (approximately 90 %; Ackerman et al., 2005, and RMC, 2011).

Finally, the runoff ratio from the Region III archetype is 0.17, slightly higher than the mean (0.13), but within the observed range from the region's watersheds (Table 5). The long-term rainfall–runoff observations for watersheds within Region III (Fig. 3f) generally follow the fit line from the archetypal watershed for dry, normal and wet years. Sweetwater River watershed experiences higher runoff ratios during wetter years than the model archetype. This is more likely due to a much higher urbanization extent (85 %) than the archetypal system (22 %) or flow alterations due to two dams within the lower portion of the watershed (Inman and Jenkins, 1999).

3.3 Archetypal evaluation: baseline period sediments

The second-order rating curves generated from observations within each respective region reside within the 95 %

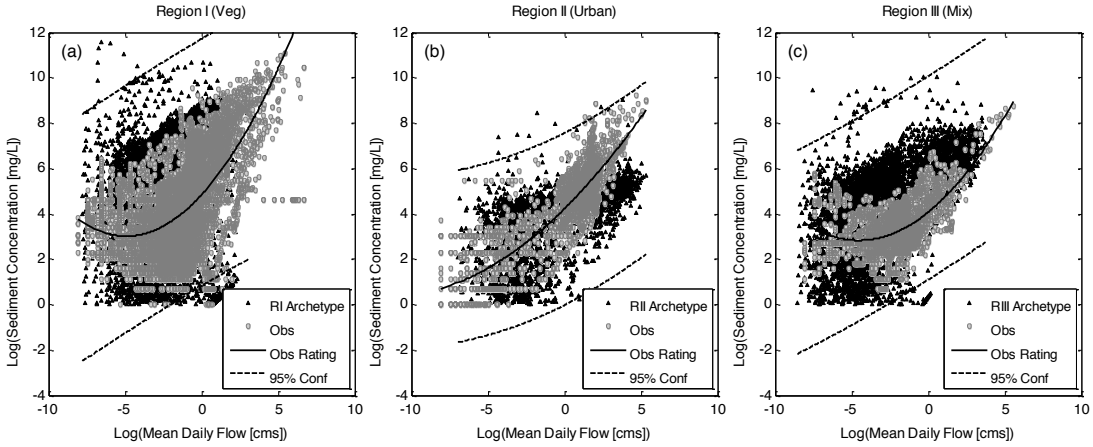

Fig. 4. Solid lines are the log(suspended sediment) rating curves (second order) for observed sites within **(a)** Region I, **(b)** Region II and **(c)** Region III. Dashed lines are the ±95 % confidence intervals for the simulated log(suspended sediment) rating curves

confidence intervals from the archetypal watersheds (Fig. 4). The rating curve from Region III's archetypal system closely matches the observations; however, sediment comparisons for this region should be interpreted cautiously given there is limited availability of sediment data. Santa Margarita (1978 WY), San Dieguito (1984 WY) and San Diego-Fashion (1984 WY) streams had only 365 days of available sediment data. Long-term sediment loads from each system were also compared to literature values and found reasonable comparisons.

The mean annual sediment fluxes for the archetypal watersheds are 2.83×10^6 ton yr^{-1}, 3.66×10^5 ton yr^{-1} and 6.13×10^5 ton yr^{-1} for the 50 yr simulation period for Regions I, II and III, respectively. Sediment observations were unavailable for the entire simulation period, but simulations from each archetype were compared to values produced by Inman and Jenkins (1999; Table 6). Mean annual sediment flux from Region I's archetypal watershed is higher than the regional average but does reside within the range of observations. Similarly, the urban archetypal watershed (Region II) provides a reasonable comparison to sediment observations. This system behaves like an urbanized system, with lower annual sediment fluxes in comparison to the other two archetypal systems. Region III's sediment flux falls within observations, but is higher than the average of the observations. As previously mentioned the lower portion of the Sweetwater River watershed is governed by two dams, likely affecting both the hydrologic and sediment flux in the system. Final parameters derived through these regional comparisons (Tables 2 and 3) were then used in each archetypal model to evaluate climate sensitivity as described below.

3.4 Runoff evaluation: temperature increase

Percent deviation in flow (change from observations to simulations) was evaluated during the baseline period to highlight archetypal system sensitivity to increasing temperatures. An increase in temperatures lowered overall simulated discharge in all three systems (Fig. 5), but the vegetated and mixed vegetated systems exhibit more sensitivity to changes in temperature than the urban archetype. In all systems, the largest loss occurs during the driest months (June–August). Temperature increase alone has minimal effect on peak discharge for all systems. Only the vegetated system experienced very minor (0–7 %) reductions in peak discharge for low-flow events (recurrence interval < 20 yr), and no changes to extreme storm events.

Flow loss due to 0.5 and 3 °C temperature increases was estimated by comparing cumulative flow depths for the 50 yr period. Cumulative flow depths for the three archetypal systems are 199, 885 and 226 cm for Regions I, II and III, respectively. The cumulative flow losses over the 50 yr period due to a 0.5 °C temperature increase are 1.5, 0.9 and 0.3 cm for Region I, II and III's archetypes, respectively. Cumulative flow losses due to a 3 °C increase are 8.4, 5.1 and 1.9 cm, respectively. Compared to total flow for the baseline period, the cumulate flow losses due to a temperature increase are not significant.

3.5 Runoff evaluation: temperature increase and precipitation variability

As expected, flow simulations resulting from the combined inputs of precipitation variability and increasing temperature exhibit greater sensitivity than simulations with temperature alone. The addition of precipitation variability causes fluctuations in mean monthly flow during the winter and spring periods, and temperature increase impacts summer flows.

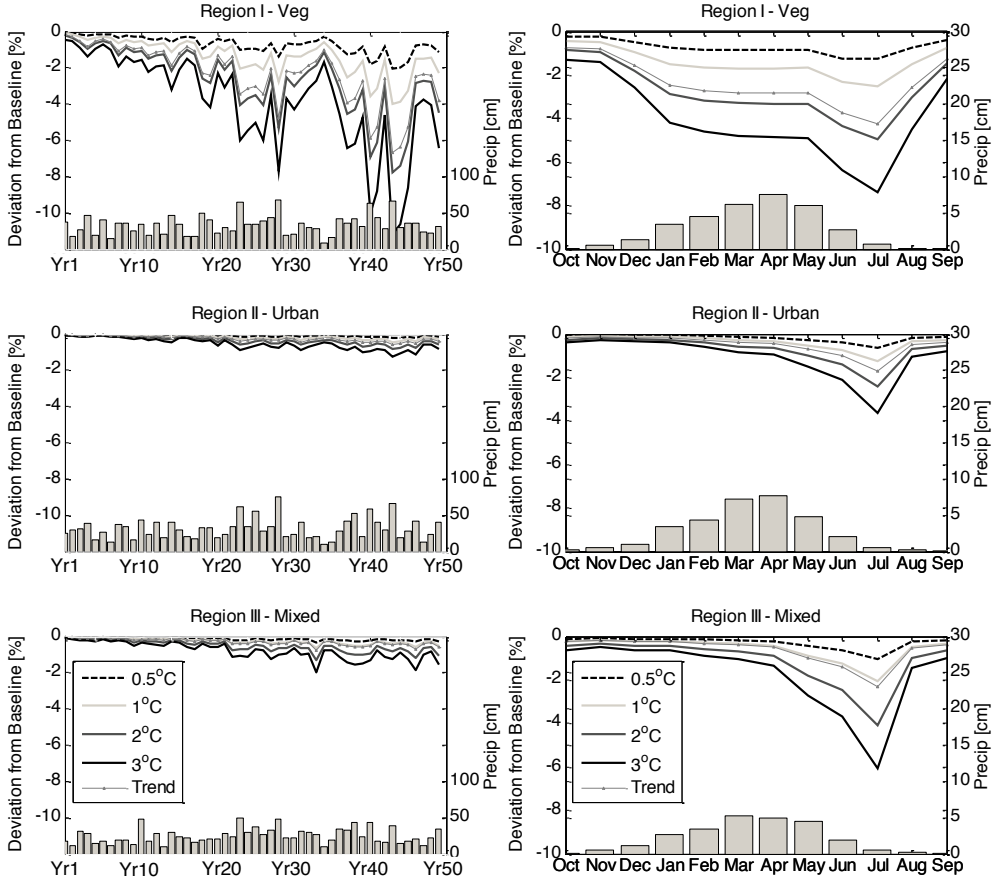

Fig. 5. Percent change in total annual flow (left) and mean monthly flow (right) from baseline simulations for the 50 yr increasing temperature scenarios only. The bottom bar graphs are the total annual precipitation (left) and mean monthly precipitation (right) used for each region. These temperature increase scenarios had no change in baseline precipitation.

Precipitation variability is also the primary variable driving the changes to peak discharge and total annual storm volume. Changes in peak discharge and annual storm volume for two return periods that coincide with low-flow (2 yr recurrence interval) and high-flow (35 yr recurrence interval) points were evaluated within the 50 yr period (Fig. 6). The upper and lower limits of the shaded region primarily correspond to results from the extreme low (5 %) and high (50 %) changes to precipitation variability.

Peak discharge for the vegetated archetype showed less sensitivity to precipitation variability than the urban and mixed systems for the 2 yr recurrence interval. The vegetated archetype experienced a −5 to 17 % deviation (from 22 cm s^{-1}) in peak discharge (Fig. 6). The deviation ranges for peak discharge were −8 to 32 % (from 590 cm s^{-1}) for Region II, and −5 to 25 % (from 121 cm s^{-1}) for Region III. These changes in low-flow behavior, especially the increase in peak flow, cause a slight shift in the recurrence intervals. Deviation ranges for Region I–III's archetypal watersheds for the 35 yr recurrence interval ranged from 4 to 92 % (from 46 cm s^{-1}), 5 to 104 % (from 1817 cm s^{-1}) and 6 to 120 % (from 280 cm s^{-1}), respectively. The deviations are significant in all systems. The lower end of the deviations in the 35 yr recurrence interval flows are due to only a 5 % precipitation variability and 3 °C temperature increase. The maximum peak discharge deviation (due to 50 % variability and 0.5 °C temperature increase) from all systems results in peak values outside the baseline range.

The 10, 25, 50, 75 and 90 % probability peak flow values in each archetypal system were identified and then evaluated for each precipitation variability scenario at 2, 5 and 35 yr recurrence intervals. In the vegetated system, high-frequency storms appear more sensitive to 5 and 10 % precipitation variability; further increase in precipitation uncertainty has little effect on peak discharge. The low-frequency storms in the vegetated system show little deviation in peak discharge due to varying precipitation. The urbanized and mixed systems are predominately governed by precipitation variability with no change due to temperature increase alone. Peak discharge distribution in the urban system widens for low-frequency storm events, but for high-frequency storms there are only minor changes. The mixed system experiences

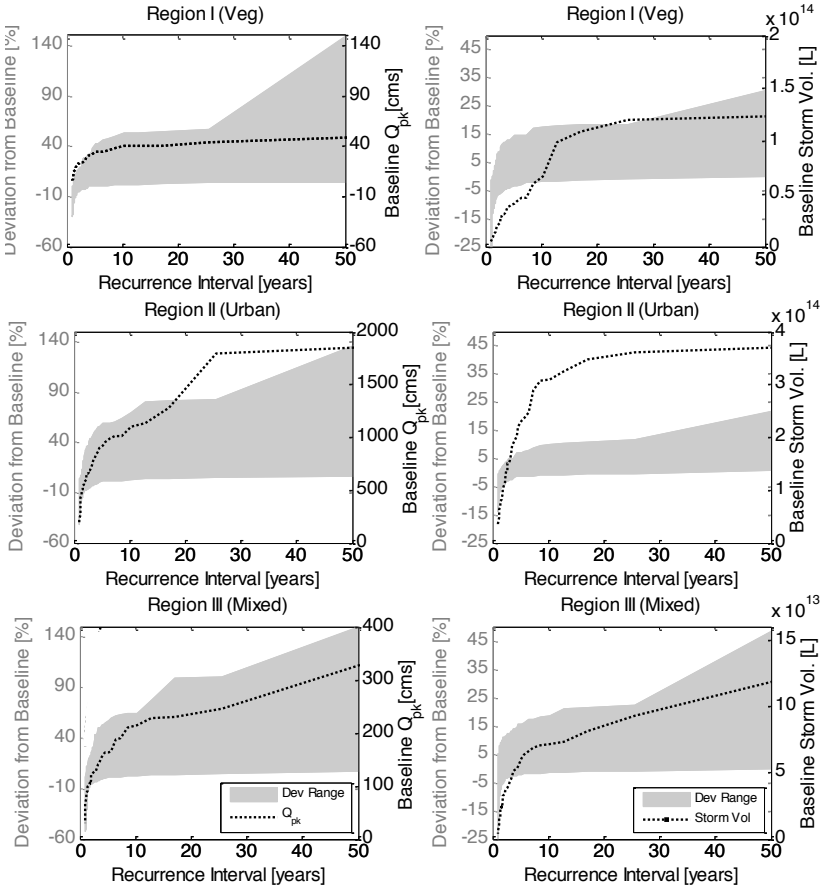

Fig. 6. Recurrence interval of peak discharge (left) and total storm volume (right) due to precipitation variability and temperature increase. Left axis corresponds to the range in percent deviation (shaded area) in peak discharge (Q_{pk}) and storm volume due to precipitation variability and temperature increase. Right axis corresponds to the baseline simulation of storm peak discharge and total storm volume (dotted line).

changes to peak discharge during both the low- and high-frequency storms.

Changes in storm volume response are enhanced in systems with more vegetated land cover. System deviations in total annual storm volume for the 2 yr recurrence interval are -7 to 6 % (from 2×10^{13} L), -5 to 3 % (from 1×10^{14} L) and -5 to 11 % (from 3×10^{13} L), for Regions I, II and III, respectively (Fig. 6). The absolute quantity in storm volume from the vegetated system is less than the urban and mixed systems; however, the percent deviation from baseline is much larger. Evaluating the 35 yr recurrence interval, the least extreme climate scenario (5 %, 0.5 °C) caused virtually no change to annual storm volume in all systems. The deviation ranges for Region I, II and III are 0 to 23 % (from 1×10^{14}), 0 to 16 % (from 4×10^{14}) and -1 to 32 % from (1×10^{14}), respectively.

3.6 Sediment evaluation: temperature increase

Given the observed sensitivity of low-flow regimes in the streamflow analysis, sediment evaluation was focused on daily concentrations and annual storm sediments during low-flow periods. Low flows were classified as those with 90 % probability of exceedance using the Weibull probability distribution for each archetype (not shown). As previously discussed, temperature increases are expected to cause a reduction in daily flow during dry periods. This results in an increase in daily suspended sediment concentrations. With projected temperature increases of 0.5 and 3 °C, the maximum increases in suspended sediment are 112 to 600 %, respectively, within the vegetated system and 59 to 283 % within the mixed archetypal watershed, respectively (Fig. 7a–c). The maximum increase in suspended sediment due to 0.5 and 3 °C temperature increases within the urban system was 17 and 38 %, respectively.

Annual storm sediments within the urban archetypal watershed exhibit minor changes with temperature increases

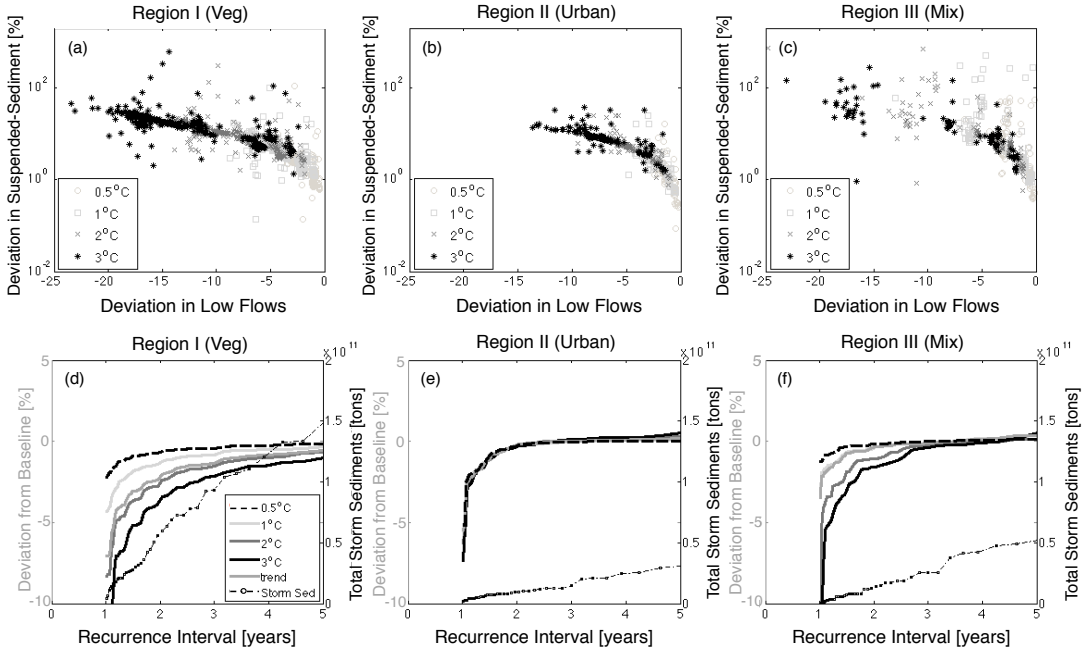

Fig. 7. Percent deviation in daily suspended sediment versus percent deviation in daily low-flow **(a–c)** and recurrence interval of annual storm sediments due temperature increase during low flow **(d–f)**. Low flow corresponds to 90 % probability of exceedance.

(Fig. 7d–f). The 2 yr recurrence interval is altered only −0.3 to 0.2 % (from 9.6×10^9 tons) within the urban archetype. The ranges of deviation for the 2 yr recurrence interval are −3 to −0.6 % (from 6×10^{10} tons) and −1.5 to −0.2 % (from 1.4×10^{10} tons) for the vegetated and mixed archetypal watersheds, respectively. It is suspected that the alterations in flow volumes were not significant enough to alter the annual suspended-sediment concentrations in any of the modeled archetypal watersheds.

3.7 Sediment evaluation: temperature increase and precipitation variability

Cumulative distribution functions of annual sediment flux (load per unit time) were examined due to climate variability; extreme (10, 90 % probability) and average (50 % probability) sediment flux from each region were compared. The urban system experienced marginal sensitivity to the climate scenarios during years characterized by low sediment flux at 10 % probability of occurrence. The vegetated and mixed systems, however, show changes in sediment flux from −5 to 8 % and −15 to 46 %, respectively. The mixed system exhibits a wider deviation because the impervious land cover enhances runoff, whereas the pervious land cover provides a sediment source. When temperature and precipitation changes are combined, both surfaces likely show an increase in sediment flux. For an average year, the mixed system again has a wider distribution than the vegetated and urban archetypes. A relative increase in sediment flux of 13 %, 4 % and 34 % was noted for Regions I, II and III, respectively. The years characterized by high sediment flux (90 % probability) caused a larger increase in the urban system by 39 %, than the vegetated (2 %) and mixed (8 %) archetypes.

Finally, long-term changes to annual storm sediment loads (tons) due to temperature increase and precipitation variability were evaluated (Fig. 8). The deviation range for the 2 yr recurrence interval for Regions I, II and III is −8 to 13 % (from 6×10^{10}), −5 to 11 % (from 10^{10}) and −7 to 33 % (from 1.4×10^{10}), respectively. Storm sediments from the vegetated and mixed systems are impacted more than the urban system during low-flow periods. As previously discussed, the urban system experienced increased sensitivity to peak discharge due to temperature increase and precipitation variability during extreme storm events. Increased wash-off of sediments from the surface is caused by enhanced peak discharge. Annual storm sediment deviations from the 35 yr recurrence interval are 1.3 to 80 % (from 5×10^{11}), 1 to 192 % (from 6.4×10^{10}) and 1 to 116 % (from 10^{11}), respectively, for Regions I, II and III.

4 Discussion

The current study utilizes a novel framework based on regional archetypal watersheds to elucidate and quantify potential impacts from climate variability on runoff and sediment fluxes in southern California. Regional archetypal watersheds were developed that closely matched observed

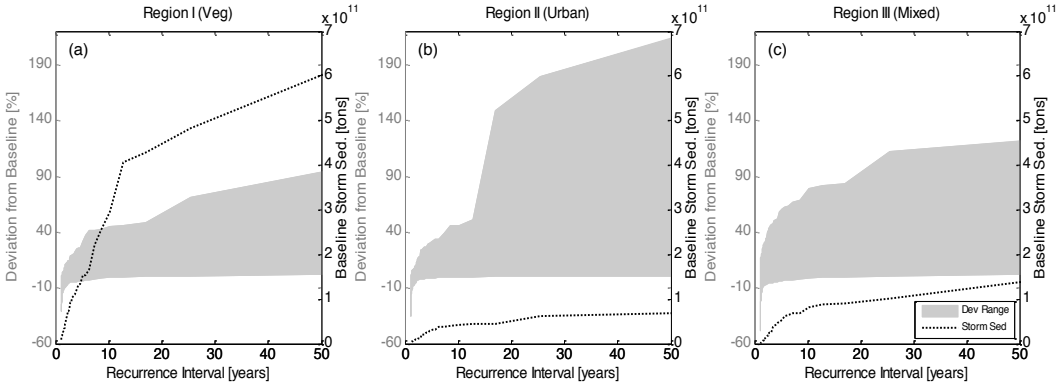

Fig. 8. Recurrence interval of annual storm sediments due temperature increase and precipitation variability. Left axis corresponds to the range in percent deviation (shaded area) in storm sediments. Right axis corresponds to the baseline simulation of storm sediments (dotted line) for **(a)** Region I, **(b)** Region II and **(c)** Region III.

Table 6. Historical comparison of mean annual sediment flux [ton yr^{-1}] for observed and archetypal watersheds for the 1969–1995 data period. Mean annual sediment flux values were obtained from Inman and Jenkins (1999).

	River	Mean annual suspended sediment flux [10^6 ton yr^{-1}] [1969–1995][a]
1	Calleguas	0.98
2	Malibu	1.14
3	Santa Clara – Montalvo, CA[b]	6.61
4	Santa Ynez	3.49
5	Ventura	0.83
	Average	2.61
	RI (Veg) Archetype	3.16
1	Ballona	0.02
2	Los Angeles – Long Beach	0.40
3	Santa Ana	0.93
	Average	0.45
	RII (Urban) Archetype	0.38
1	San Diego – Santee	0.02
2	San Luis Rey	0.88
3	Santa Margarita	0.18
4	Sweetwater	0.01
	Average	0.27
	RIII (Mix) Archetype	0.77

[a] Taken from Inman and Jenkins (1999); [b] different Santa Clara gauge location – station ID 11114000.

hydrologic and sediment behavior. Vegetation and urbanization extent heavily influenced sensitivity in future flow and sediment fluxes, as reflected by the three archetypal systems.

Temperature increase only will primarily affect the more vegetated watersheds within southern California, especially during the low-flow season. Minimal change was noted for storm volume and peak discharge. The loss in flow is likely due to increased evapotranspiration rates from soil and vegetated surfaces, reducing channel flow in the spring and summertime. During low-flow periods (90 % probability of exceedance) there is a significant increase in daily sediment concentration in the vegetated and mixed vegetated-urban systems. Sediment inundation due to temperature increase has been noted in previous studies within the Sierra Nevada (Hayhoe et al., 2004; Mote et al., 2005), the Colorado River basin (Gleick and Chalecki, 1999; Christensen et al., 2004; McCabe and Wolock, 2008) and the State Water Project and Central Valley (Vicuna et al., 2007). An increase in suspended-sediment concentration is expected to have significant implications for downstream ecosystems. Wetlands, lagoons and estuaries are reliant on upstream inflow and sediment fluxes. Seasonal alterations to temperature affect inlet flow, sediment and contaminant concentrations, which are important driving factors influencing wetland removal of contaminants (Kadlec and Reddy, 2001).

Combined precipitation variability as well as temperature increase affects all archetypal watershed's peak storm discharge and annual flow volumes. Urbanization extent plays an important role in the sensitivity of the system. The highly urbanized systems are expected to experience an enhancement in peak storm discharge primarily due to precipitation variability. This will cause a shift in recurrence intervals, where the urban system will experience previously categorized high-flow events at a lower recurrence interval (i.e., a 17 yr storm may occur at a 10 yr interval due to 50 % precipitation variability and 0.5 °C temperature increase in Region II) and infrequent storm events with a higher recurrence interval will be more extreme. In response, it is anticipated that an increase in storm sediments due to enhanced scour and wash-off from pockets of pervious surfaces within an

urban environment. Urban expansion is known to have an effect on urban runoff that carries sediment and other hazardous materials such as trash, motor oil, fertilizers, animal waste, etc. (Wolman, 1967; Trimble, 1997; ASCE, 2006; Warrick and Rubin, 2007). This was evident in Region III's mixed archetypal watershed. The vegetation and urban extent with the mixed archetype caused a dual affect: the impervious/urban land cover increased peak discharge and storm volume and the pervious/vegetated land cover provided a sediment source increasing sediment concentrations.

Our work corroborates previous studies and, in addition, provides relative quantification of change that will result from a range of climate scenarios developed within each region. Given extreme precipitation patterns, the lack of infiltration capacity in highly developed and mixed developed systems may potentially exacerbate flooding hazards and stress the region's aging infrastructure. The City of Los Angeles Infrastructure Report Card states the storm water facilities, including open channels, corrugated metal pipes, vitrified clay pipes and other devices, are currently grade C+ (A being the best and F being the worst) (Troyan, 2003). Approximately 48 % of the system was built 20 to 50 yr ago and assumed to have minimal defects, and 41 % was built 50 to 80 yr ago and assumed to have moderate structural defects (Troyan, 2003). In 2003, the city's storm water system was also noted as deficient in capacity because it could not handle flows generated by a 10 yr storm (Troyan, 2003). Given the findings from this project, climate variability may significantly challenge the capacity of the storm water infrastructure in the city.

5 Concluding remarks

The significance of our findings relies on investigating each regional system's ability to adapt to changes in flow and sediment regimes due to predicted climate variability. The developed archetypal watersheds are meant to investigate and quantify *relative change* based on land cover and can be scaled to consider specific (real) watershed systems. Precipitation, temperature, geological formation and land cover are key factors that affect runoff and sediment yield (Warrick and Mertes, 2009; Inman and Jenkins, 1999). Our approach allows the user to test regional sensitivity to each factor to determine the expected range of deviation in flow and sediment yield and can be scaled to focus on individual watershed analysis.

The methods presented in our study provide an alternative approach to evaluate change in flow and sediment flux due to theoretical future temperature and precipitation scenarios across regional scales. By comparing regional simulations to observations it is possible to validate the usability of our quasi-synthetic systems and provide a reasonable assessment of long-term perturbations to flow and sediment due to varying climate. The developed method was tested using synthetic scenarios with potential change estimated from the IPCC or the literature; this approach was used to validate the usefulness of the method and can be further explored using other model-based scenarios.

The developed approach can also be expanded by using other rainfall–runoff models, high-resolution land cover datasets, alternative approaches to developing climate scenarios and altering future land cover. Our purpose was to develop a method that can be used in other regions or for specific watersheds where an extensive dataset (physiological, meteorological, hydrologic, sediment) may not available. The advocated benefits of using the developed archetypal watershed approach include the following:

- User-defined regional classification where user can subcategorize within vegetated and urban regions.
- Minimal need for basin-specific meteorological data.
- Significant potential for application to ungauged (non-instrumented) systems.
- Quantification of sediment and streamflow changes that can be used to investigate impacts on a range of sensitive downstream ecosystems and infrastructure.
- The ability to investigate multiple climate scenarios with relative ease due to minimal necessary calibration parameters.
- The ability to aggregate watershed effects to look for regional patterns and potential effects on specific coastal systems, including the Southern California Bight.

Future work includes investigating potential environment effects on downstream estuaries due to changing hydrologic and sediment fluxes. Additional work is likely needed to assess the impacts of climate change on nutrient and metal transport from coastal watersheds to downstream aquatic ecosystems. Future analysis will also focus on changes in extent and distribution of aquatic ecosystems due to changes in terrestrial (flow, sediment, contaminants) as well as oceanic forcing (salt-water intrusion).

Acknowledgements. This work was funded by the California State Water Board (#06-241-250), the Southern California Coastal Water Research Project (SCCWRP), a National Science Foundation Graduate Research fellowship (DGE #0707424) and an NSF CAREER grant (#EAR0846662). Special thanks to Drew Ackerman for guidance on the HSPF modeling for this project.

Edited by: B. McGlynn

References

Ackerman, D., Schiff, K. C., and Weisberg, S. B.: Evaluating HSPF in an Arid, Urbanized Watershed, J. Am. Water Resour. As., 41, 477–486, 2005.

American Society of Civil Engineers (ASCE): California Infrastructure Report Card: A Citizen's Guide, available at: http://www.ascecareportcard.org/Citizen_guides/2006_citizens_guide.pdf (last access: December 2007), 2006.

Aragão, L. E. O. C., Malhi, Y., Roman-Cuesta, R. M., Saatchi, S., Anderson, L. O., and Shimabukuro, Y. E.: Spatial patterns and fire response of recent Amazonian droughts, Geophys. Res. Lett., 34, L07701, DOI:10.1029/2006GL028946, 2007.

Bandurraga, M., Rindahl, B., and Butcher, J.: Use of HSPF for Design Storm Modeling in Semi-Arid Watersheds, ASCE Conference Proceedings, 414, 4579–4586, 2011.

Bicknell, B., Imhoff, J. C., Kittle, J. L., Jobes, T. H., and Donigian, A. S.: Hydrological Simulation Program–Fortran (HSPF): User's Manual for Release 12, US Environmental Protection Agency: Athens, GA, 2000.

California Climate Change Center (CCCC): Our Changing Climate—Assessing the Risks to California, available at: http://www.climatechange.ca.gov/biennial_reports/2006report/index.html (last access: 15 November 2007), 2006.

California Department of Conservation – Division of Land Resource Protection: Farmland Mapping and Monitoring Program, available at: http://redirect.conservation.ca.gov/DLRP/fmmp/county_info_results.asp (last access: June 2012), 2011.

California Department of Finance: Population Projections for California and Its Counties 2000–2050, by Age, Gender and Race/Ethnicity, Sacramento, California, July 2007, 2007.

Christensen, N. S., Wood, A. W., Voisin, N., Lettenmaier, D. P., and Palmer, R. N.: The Effects of Climate Change on the Hydrology and Water Resources of the Colorado River Basin, Climatic Change, 62, 337–363, 2004.

Clark, G. M.: Changes in Patterns of Streamflow from Unregulated Watersheds in Idaho, Western Wyoming, and Northern Nevada, J. Am. Water. Resour. As., 46, 486–497, 2010.

Climate action team (CAT): Biennial Report, March 2009, available at: http://www.energy.ca.gov/2009publications/CAT-1000-2009-003/CAT-1000-2009-003-D.PDF (last access: 10 October 2010), 2009.

Costa, A. C. and Soares, A.: Trends in extreme precipitation indices derived from a daily rainfall database for the South of Portugal, Int. J. Climatol., 29, 1956–1975, 2009.

Department of Water Resources (DWR): Climate Change Report – Progress on Incorporating Climate Change into Management of California's Water Resources Technical Memorandum Report, available at: http://baydeltaoffice.water.ca.gov/climatechange.cfm (last access: 16 January 2010), 2006.

DeWalle, D. R., Swistock, B. R., Johnson, T. E., and Maguire, K. J.: Potential Effects of Climate Change and Urbanization on Mean Annual Streamflow in the United States, Water Resour. Res., 36, 2655–2664, 2000.

Donigian, A. S. and Love, J. T.: Sediment Calibration Procedures and Guidelines for Watershed Modeling, Water Environ. Feder., 20, 728–747, 2003.

Githui, F., Gitau, W., Mutua, F., and Bauwens, W.: Climate change impact on SWAT simulated streamflow in western Kenya, Int. J. Climatol., 29, 1823–1834, doi:10.1002/joc.1828, 2009.

Gleick, P. H. and Chalecki, E. L.: The Impacts of Climate Changes for Water Resources of the Colorado and Sacramento-San Joaquin River Basins, J. Am. Water Resour. As., 35, 1429–1441, 1999.

Goff, K. M. and Gentry, R. W.: The influence of watershed and development characteristics on the cumulative impacts of stormwater detention ponds, Water Resour. Manag., 20, 829–860, 2006.

Hack, J. T.: Studies of Longitudinal Profiles in Virginia and Maryland, US Geological Survey Professional Papers, Vol. 294-B, 45–97, 1957.

Hayhoe, K., Cayan, D., Field, C. B., Frumhoff, P. C., Maurer, E. P., Miller, N. L., Moser, S. C., Schneider, S. H., Cahill, K. N., Cleland, E. E., Dale, L., Drapek, R., Hanemann, R. M., Kalkstein, L. S., Lenihan, J., Lunch, C. K., Neilson, R. P., Sheridan, S. C., and Verville, J. H.: Emissions Pathways, Climate Change, and Impacts on California, P. Natl. Acad. Sci. USA, 101, 12422–12427, 2004.

He, M. and Hogue, T. S.: Integrating Hydrologic Modeling and Land Use Projections for Evaluation of Hydrologic Response and Regional Water Supply Impacts in Semi-arid Environments, Environ. Earth Sci., 65, 1671–1685, 2011.

Hevesi, J. A., Flint, L. E., Church, C. D., and Mendez, G. O.: Application of a watershed model (HSPF) for evaluating sources and transport of pathogen indicators in the Chino Basin drainage area, San Bernardino County, California, US Geological Survey Scientific Investigations Report 2009-5219, 146 pp., 2011.

Hidalgo, H. G., Das, T., Dettinger, M. D., Cayan, D. R., Pierce, D. W., Barnett, T. P., Bala, G., Mirin, A., Wood, A. W., Bonfils, C., Santer, B. D., and Nozawa, T: Detection and Attribution of Streamflow Timing Changes to Climate Change in the Western United States, J. Climate, 22, 3838–3855, 2009.

Inman, D. and Jenkins, S.: Climate: Change and the Episodicity of Sediment Flux of Small California Rivers, J. Geology, 107, 251–270, 1999.

Intergovernmental Panel on climate Change (IPCC): Climate Change, 2001, Special Report on Emission Scenarios, Contribution of Working Group I to the Third Assessment Report of the Intergovernmental Panel on Climate Change, edited by: Nakicenovic, N. and Swart, R., Cambridge University Press, Cambridge United Kingdom and New York, NY, USA, 2001.

Intergovernmental Panel on climate Change (IPCC): Climate Change 2007: Synthesis Report. Contribution of Working Groups I, II and III to the Fourth Assessment Report of the Intergovernmental Panel on Climate Change, edited by: Pachauri, R. K. and Reisinger, A., IPCC, Geneva, Switzerland, 104 pp., 2007.

Kadlec, R. H. and Reddy, K. R.: Temperature Effects in Treatment Wetlands Water Environment Research, Water Environ. Feder., 73, 543–557, 2001.

Kim, J.: A projection of the effects of climate change induced by increased CO_2 on extreme hydrologic events in the western US, Climatic Change, 68, 153–168, 2005.

Kiparsky, M. and Gleick, P. H.: Climate Change and California Water Resources: A Survey and Summary of the Literature, Pacific Institute for Studies in Development, Environment, and Security, Oakland, CA,, 2003.

Knowles, N. and Cayan, D. R.: Potential Effects of Global Warming on the Sacramento/San Joaquin Watershed and the San Francisco Estuary, Geophys. Res. Lett., 29, 38-1–38-4, 2002.

Kunkel, K. E., Palecki, M., Ensor, L., Hubbard, K. G., Robinson, D., Redmond, K., and Easterling, D.: Trends in twentieth-century U.S. snowfall using a quality-controlled dataset, J. Atmos. Ocean Tech., 26, 33–44, 2009.

Levien, L., Fischer, C., Parks, S., Maurizi, B., Suero, J., Mahon, L., Longmire, P., and Roffers, P.: Monitoring land cover changes in California, a USFS and CDF cooperative program, South Coast Project Area, State of California, Resources Agency, Department of Forestry and Fire Protection, Sacramento, CA, 2002.

Los Angeles Department of Water and Power (LADWP): Urban Water Management Plan 2010, available at: www.ladwp.com (last access: March 2013), 2010.

Manguerra, H. B. and Engel, B. A.: Hydrologic parameterization of watersheds for runoff prediction using SWAT, J. Am. Water Resour. As., 34, 1149–1162, 1998.

McCabe, G. J. and Wolock, D. M.: Warming and Implications for Water Supply in the Colorado River Basin, in: World Environmental and Water Resources Congress 2008, Ahupua'a, ASCE, 273, 1–10, 2008.

Meehl, G.A., Zwiers, F., Evans, J., Knutson, T., Mearns, L., and Whetton, P.: Trends in extreme weather and climate events: issues related to modeling extremes in projections of future climate change, B. Am. Meterol. Soc., 81, 427–436, 2000.

Miller, N. L., Bashford, K. E., and Strem, E.: Potential impacts of climate change on California hydrology, J. Am. Water. Resour As., 39, 771–784, 2003.

Moradkhani, H., Hsu, K. L., Gupta, H., and Sorooshian, S.: Uncertainty assessment of hydrologic model states and parameters: Sequential data assimilation using the particle filter, Water Resour. Res., 41, W05012,doi:10.1029/2004WR003604, 2005.

Mote, P. W., Hamlet, A. F., Clark, M. P., and Lettenmaier, D. P. Declining mountain snowpack in western North America, B. Am. Meterol. Soc., 86, 39-49, 2005.

National Oceanographic and Atmospheric Administration-Coastal Services Center (NOAA-CSC): Southern California 2000-Era Land Cover/Land Use, LANDSAT-TM, 30m, NOAA-CSC, Charleston, SC, available at: http://www.csc.noaa.gov/crs/lca/pacificcoast.html (last access: 1 July 2007), 2003.

National Oceanographic and Atmospheric Administration – National Weather Service (NOAA-NWS): Climate Prediction Center Cold and Warm Episodes by Season, available at: http://www.cpc.noaa.gov/products/analysis_monitoring/ensostuff/ensoyears.shtml (last access: 20 December 2010), 2010.

Nearing, M. A., Jetten, V., Baffaut, C., Cerdan, O., Couturier, A., Hernandez, M., Le Bissonnais. Y., Nichols, M. H., Nunes, J. P., Renschler, C. S., Souchere, V., and van Oost, K.: Modeling response of soil erosion and runoff to changes in precipitation and cover, Catena, 61, 131–154, 2005.

Nezlin, N. P. and Stein, E. D.: Spatial and temporal patterns of remotely-sensed and field-measured rainfall in southern California, Remote Sens. Environ., 96, 228–245, 2005.

Pataki, D. E., Boone, C. G., Hogue, T. S., Jenerette, G. D., McFadden, J. P., and Pincetl, S.: Socio-ecohydrology and the urban water challenge in the western U.S., Ecohydrology, 4, 341–347, 2011.

Payne, J. T., Wood, A. W., Hamlet, A. F., Palmer, R. N., and Lettenmaier, D. P.: Mitigating the Effects of Climate Change on the Water Resources of the Columbia River Basin, Climatic Change, 62, 233–256, 2004.

Philips, J. R.: The theory of infiltration: the infiltration equation and its solution, Soil Sci., 83, 345–375, 1957.

Pruski, F. F. and Nearing, M. A.: Climate-induced changes in erosion during the 21st century for eight U.S. locations, Water Resour. Res., 38, 1298–1309, 2002.

Rind, D., Goldberg, R., and Ruedy, R.: Change in Climate Variability in the 21st Century, Climatic Change, 14, 5–37, 1989.

River and Mountains Conservancy (RMC): San Gabriel & Lower Los Angeles, Rio Hondo Watershed Management Plan, available at: http://www.rmc.ca.gov/plans/rio_hondo/Rio%20Hondo%20Water%20Management%20Plan_small.pdf (last access: June 2011), 2011.

Singer, M. B. and Dunne, T.: An empirical-stochastic, event-based model for simulating inflow from a tributary network: Theoretical framework and application to the Sacramento River basin, California, Water Resour. Res., 40, W07506, doi:10.1029/2003WR002725, 2004.

Singh, J., Knapp, H. V., Arnold, J. G., and Demissie, M.: Hydrological modeling of the Iroquois river watershed using HSPF and SWAT, J. Am. Water Resour. As., 41, 343–360, 2005.

Smith, J. and Eli, R. N.: Neural-network models of rainfall-runoff process, J. Water Res. Pl.-ASCE, 121, 499–508, 1995.

Soboll, A., Elbers, M., Barthel, R., Schmude, J., Ernst, A., and Ziller, R.: Integrated regional modelling and scenario development to evaluate future water demand under global change conditions, Mitigation Adapt. Strategies Global Change, 16, 477–498, 2011.

Trimble, S.: Sediment Yield from an Urbanizing Watershed Contribution, Science, 278, 1442–1444, 1997.

Troyan, V. B.: Infrastructure report card for the city of Los Angeles: Executive Summary. Bureau of Engineering, Department of Public Works, available at: http://eng.lacity.org/bureau_docs/Complete_Exec_Summary.pdf (last access: November 2011), 2003.

US Environmental Protection Agency (EPA): Better Assessment Science Integrating Point and Non-point Sources, available at: http://www.epa.gov/waterscience/basins/ (last access: 20 December 2010), 2007.

US Geological Survey (USGS): Suspended-Sediment Database Daily Values of Suspended Sediment and Ancillary Data, available at: http://co.water.usgs.gov/sediment/ (last access: 10 January 2011), 2009.

US Geological Survey (USGS): USGS Surface-Water Data for USA, available at: http://waterdata.usgs.gov/nwis/sw (last access: 9 September 2011), 2011.

Vicuna, S., Maurer, E. P., Joyce, B., Dracup, J. A., and Purkey, D.: The Sensitivity of California Water Resources to Climate Change Scenarios, J. Am. Water Resour. As., 43, 482–498, 2007.

Wang, J. H., Hong, Y., Gourley, J., Adhikari, P., Li, L., and Fengge, S.: Quantitative assessment of climate change and human impacts on long-term hydrologic response: a case study in a subbasin of the Yellow River, China, Int. J. Climatol., 30, 2130–2137, 2010.

Warrick, J. A. and Mertes, L. A. K.: Sediment yield from the tectonically active semiarid Western Transverse Ranges of California, Geol. Soc. Am. Bull., 121, 1054–1070, doi:10.1029/2006JF000662, 2009.

Warrick, J. A. and Rubin, D.: Suspended-sediment rating-curve response to urbanization and wildfire, Santa Ana River, California, J. Geophys. Res. Earth Surf., 112, F02018, doi:10.1029/2006JF000662, 2007.

Westerling, A. L. and Bryant, B. P.: Climate change and wildfire in California, Climatic Change, 87, S231–S249, 2008.

Wolman, M. G.: A Cycle of Sedimentation and Erosion in Urban River Channels, Geograf. Ann. Ser. A, 49, 385–395, 1967.